J|A|C|S COMMUNICATIONS

Published on Web 11/26/2004

Insights into the Spin-Forbidden Reaction between L_2Pd^0 and Molecular Oxygen

Clark R. Landis,* Christine M. Morales, and Shannon S. Stahl*

Department of Chemistry, University of Wisconsin-Madison, 1101 University Avenue, Madison, Wisconsin 53706

Received September 2, 2004; E-mail: landis@chem.wisc.edu; stahl@chem.wisc.edu

Palladium-catalyzed reactions continue to emerge as effective methods for selective aerobic oxidation of organic molecules.[1] These reactions often proceed by a two-stage "oxidase" mechanism (Scheme 1), and recently, a number of catalyst systems have been identified that undergo efficient dioxygen-coupled turnover in the absence of cocatalysts such as $CuCl_2$.[1] These results imply that molecular oxygen reacts directly with palladium(0). We recently reported a bathocuproine-coordinated palladium(0) complex that reacts with dioxygen to produce the η^2-peroxopalladium(II) species, **1**.[2,3] This two-electron redox process involves reaction of a closed-shell Pd complex and triplet O_2 to give a closed-shell Pd−O_2 adduct.[4] To probe the electronic structural factors underlying this transformation, we have used spin-unrestricted density functional theory (DFT) to investigate reversible association of O_2 at an ethylendiamine-coordinated palladium(0) fragment, (en)Pd, **2**. Although palladium generally participates in two-electron redox reactions, this study highlights the role of one-electron steps to alleviate spin restrictions.

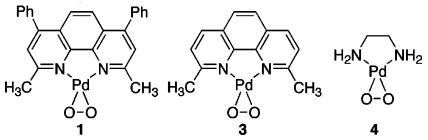

η^2-Peroxopalladium(II) analogues **3** and **4** represent models of **1** suitable for computational studies. Their relevance to experimental results is supported by the use of diverse nitrogen ligands, including saturated amines, in aerobic palladium oxidation catalysis.[5] DFT-computed bond lengths and structural parameters for **3** and **4**[6] closely match those of crystallographically characterized **1** (Table S1). The O−O bond lengths in these complexes (1.40−1.41 Å) are consistent with their formulation as palladium(II) peroxides. Addition of triplet O_2 to a singlet (N−N)Pd^0 fragment to form **3** and **4** is computed to be exothermic ($\Delta E = -41.5$ and -38.0 kcal/mol, respectively) in the gas phase. The calculated exothermicity is even higher in solution (CH_2Cl_2: $\Delta E = -50.6$ and -53.7 kcal/mol, respectively)[7] because of the polarity of (N−N)$Pd^{II}(O_2)$ complexes. Building on these thermodynamic data, we probed the trajectory of the reaction between O_2 and (en)Pd^0 to address several questions: (1) Does O_2 approach the metal side-on or end-on? (2) Is the two-electron transfer from palladium to O_2 stepwise or concerted? (3) At what stage in the mechanism does spin-crossover occur?

DFT(UB3LYP) computations were used to characterize the reaction trajectory between **2** and triplet O_2. Total energies, geometries, and charge distributions along the trajectory were obtained from relaxed potential energy scans. This reaction is exothermic and encounters no barrier along the triplet surface and results in formation of a triplet diradical, Pd^I−(η^1-superoxide) complex, ^{3}**6** (Figure 1). Triplet-to-singlet surface crossing permits formation of the η^2-peroxo complex ^{1}**4**.

Scheme 1. Two-Stage Palladium Oxidase Mechanism

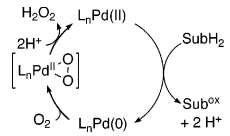

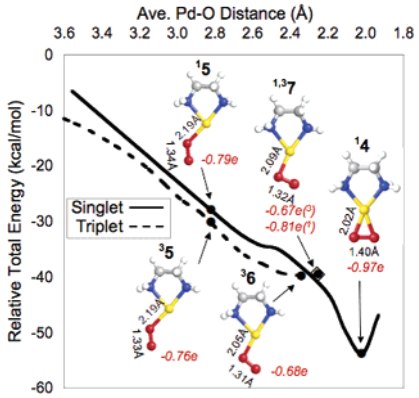

Figure 1. Singlet and triplet surfaces for the oxygenation of (en)Pd (**2**) in CH_2Cl_2, calculated with the UB3LYP functional and PCM solvent model, showing total energies relative to the ground-state energy of $^3O_2$ + (en)Pd^0, important bond lengths (Å), and natural charges of the O_2 fragment (red italics) as a function of the average Pd−O distance.

At large Pd−O distances ($r_{ave} > 5.0$ Å), exchange interaction between the unpaired electrons in dioxygen significantly stabilizes the triplet relative to the singlet surface ($\Delta E_{S-T} > 10$ kcal/mol). At intermediate distances (2.3 Å $< r <$ 4.0 Å), however, the singlet−triplet gap shrinks considerably (e.g., $\Delta E_{S-T} = 2.9$ kcal/mol at $r = 2.7$ Å). In this range, significant charge transfer occurs from palladium into the singly occupied, in-plane π^* orbital ($\pi_{||}^*$) of dioxygen.[8] The geometry and electronic structure of the (en)Pd···O_2 interaction in this region corresponds to a Pd^I−(η^1-superoxide) adduct for both spin states. For example, at $r = 2.7$ Å, both singlet and triplet structures (^{1}**5** and ^{3}**5**) exhibit bent Pd−O−O geometries (130.6° and 130.8°, respectively) and O−O bond distances elongated by 0.1 Å relative to free O_2 (Figure 1). The O_2 fragments possess a natural charge of $\sim -0.8e$ that is distributed nearly equally over the two oxygen atoms. Both ^{1}**5** and ^{3}**5** are diradicals with surprisingly similar electron density distributions (Figure 2[9]). One unpaired electron lies primarily in the superoxide π^* orbital oriented perpendicular to the N_2Pd plane ($\pi_\perp^*$) and is equally distributed over both oxygen atoms. The second unpaired electron is mostly localized in a Pd-centered s−d combination lying in the plane of the molecule. In keeping with these descriptions, the spin densities on Pd and O_2 fragments are 0.74 and 1.12, respectively, in the triplet state and 0.75 and 0.91 in the singlet state. The residual spin densities are delocalized on the en ligand. Spatial separation of the unpaired spins in these adducts mitigates

10.1021/ja044674b CCC: $27.50

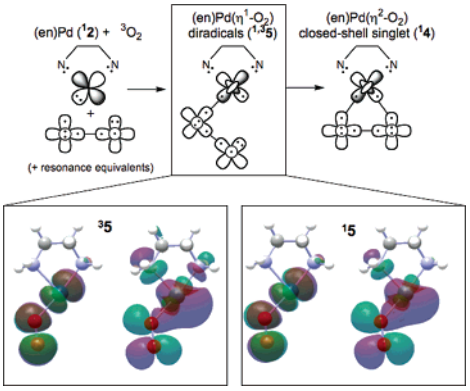

Figure 2. Evolution of the electronic structure during the oxygenation of ^{1}**2** expressed in terms of generalized valence bond Lewis-like diagrams (top) and surface plots of Kohn−Sham orbitals bearing unpaired spin density (bottom) that demonstrate the similarity of singlet and triplet states at the geometry of **5**. The Pd-centered dark and light lobes of the Lewis representations of **4** and **5** represent pairs of s−d hybridized orbitals with perpendicular, in-plane directionalities.

the stabilizing exchange interaction in the triplet state and results in similar singlet and triplet energies at these Pd−O distances.

The global minimum on the triplet surface, ^{3}**6**, at $r = 2.34$ Å is stabilized by −39.8 kcal/mol relative to the separated reactants and features an end-on Pd^{I}−superoxide structure.[10] Spin restrictions prohibit coupling of the unpaired spins to form a second Pd−O bond. The singlet diradical, however, can form a second Pd−O bond by rotating the $\pi_{\perp}$* orbital into the coordination plane. As a result, the singlet surface diverges sharply from that of the triplet at Pd−O distances of <2.3 Å. The minimum energy on the singlet surface, **4**, is stabilized by 14 kcal/mol relative to **6**. Conversion of **6** into **4** results in the formal transfer of one more electron from Pd into the O_2 fragment, which is manifested by an increase in the computed O−O bond length (1.31 vs 1.40 Å) and a decrease in the computed O−O stretching frequency (1165 vs 970 cm^{-1}).

Conversion of **6** into **4** requires intersystem crossing from the triplet to singlet reaction surfaces. This spin crossover is most probable at the minimum energy crossing point (MECP, ^{1,3}**7**), which was optimized by the method of Harvey et al.[11] at an average Pd−O distance of 2.26 Å. The transition from triplet structure **4** to the MECP is uphill by only 0.2 kcal/mol. Crossover to the singlet surface is mediated by spin−orbit coupling, which is generally large at transition-metal centers. The magnitude of the spin−orbit coupling matrix element, $\langle ^1\mathbf{7}|H_{SO}|^3\mathbf{7}\rangle$, is estimated to be 138 cm^{-1}.[12] This value, combined with the 0.2 kcal/mol activation energy to the MECP, leads to a spin crossover rate of $\sim 10^{12}$ s^{-1}. Spin crossover dynamics do not influence the overall oxygenation kinetics. We note that separated radical pairs containing superoxide ion undergo rapid triplet−singlet relaxation due to spin−orbit coupling within the superoxide ion.[13] However, this contribution to relaxation of ^{3}**7** is suppressed by the strong (en)Pd^{I}−O_2^- interaction, which quenches the orbital angular momentum of superoxide.

Discussions of O_2 reactivity with closed-shell reactants frequently consider contributions arising from the spin-forbidden nature of reactions that generate closed-shell products.[13,14] The DFT results reported here exhibit important similarities to those obtained from a recent study of the oxygenation of deoxyhemocyanin, which possesses a closed-shell binuclear Cu^{I} active site.[15] Concerted charge transfer from *both* d^{10} Cu^{I} centers to dioxygen delocalizes spin density onto the separated copper centers, thereby weakening the exchange interaction and facilitating spin crossover to yield the singlet product. In the present system, electron transfer from a *single* d^{10} Pd^0 center achieves the same result by forming a triplet diradical with one spin localized on palladium and one on O_2. These observations contradict the suggestion that palladium-catalyzed oxidation reactions employ transition-metal cocatalysts or benzoquinone to circumvent an intrinsically slow, spin-forbidden reaction between Pd(0) and O_2.[16]

Acknowledgment. Financial support is gratefully acknowledged: NSF (CAREER, CHE-0094344), Dreyfus Foundation (Teacher-Scholar Award), and the Sloan Foundation (Research Fellowship) (S.S.S.) and DOE (C.R.L.). We thank Prof. Jeremy Harvey for sharing computer routines to locate MECPs, Prof. Thomas Brunold for critical comments, and Prof. Frank Weinhold for helpful discussions.

Supporting Information Available: Computational description and tabulated data (PDF). This material is available free of charge via the Internet at http://pubs.acs.org.

References

(1) Stahl, S. S. *Angew. Chem., Int. Ed.* **2004**, *43*, 3400−3420.
(2) Stahl, S. S.; Thorman, J. L.; Nelson, R. C.; Kozee, M. A. *J. Am. Chem. Soc.* **2001**, *123*, 7188−7189.
(3) For additional examples of Pd^0 oxygenation, see: (a) Wilke, G.; Schott, H.; Heimbach, P. *Angew. Chem., Int. Ed.* **1967**, *6*, 92−93. (b) Yoshida, T.; Otsuka, S. *J. Am. Chem. Soc.* **1977**, *99*, 2134−2140. (c) Yoshida, T.; Tatsumi, K.; Matsumoto, M.; Nakatsu, K.; Nakamura, A.; Fueno, T.; Otsuka, S. *Nouv. J. Chim.* **1979**, *3*, 761−774. (d) Konnick, M. M.; Guzei, I. A.; Stahl, S. S. *J. Am. Chem. Soc.* **2004**, *126*, 10212−10213.
(4) For a recent discussion of open-shell organotransition metals reacting with closed-shell substrates to form closed-shell metal complexes, see: Carreón-Macedo, J.-L.; Harvey, J. N. *J. Am. Chem. Soc.* **2004**, *126*, 5789−5797.
(5) For representative examples, see: (a) Nishimura, T.; Onoue, T.; Ohe, K.; Uemura, S. *J. Org. Chem.* **1999**, *64*, 6750−6755. (b) ten Brink, G.-J.; Arends, I. W. C. E.; Sheldon, R. A. *Science* **2000**, *287*, 1636−1639. (c) Jensen, D. R.; Pugsley, J. S.; Sigman, M. S. *J. Am. Chem. Soc.* **2001**, *123*, 7475−7476. (d) Ferreira, E. M.; Stoltz, B. M. *J. Am. Chem. Soc.* **2001**, *123*, 7725−7726.
(6) Calculations were performed with Gaussian 98 using the UB3LYP formalism, the Stuttgart effective core representation, and triple-ζ basis set for Pd, 6-311G**$^{++}$ basis sets for all other elements, and the PCM solvent model. All computed energies were corrected for spin contamination artifacts, and computations using the BP86 functional gave similar results (see Supporting Information for further details).
(7) Experimental studies of palladium(0) oxygenation were conducted in CH_2Cl_2. In the calculations, solvent was incorporated using the PCM solvent model.
(8) The calculated ionization potential of (en)Pd^0 and electron affinity of O_2 reveal that long-range electron transfer (eq 1) is highly endothermic in the gas phase (+107 kcal/mol), but nearly thermoneutral (+3.4 kcal/mol) in CH_2Cl_2 solution. Therefore, initiation of the oxygenation reaction by outer-sphere electron transfer from **2** to O_2 differs from the pathway depicted in Figure 1 only by the presence of a small barrier at large Pd−O_2 separations.

$$(\text{en})\text{Pd}^0 + \text{O}_2 \rightarrow [(\text{en})\text{Pd}^{\text{I}}]^+ + \text{O}_2^- \quad \Delta E = \text{IP}^{\text{Pd}} + \text{EA}^{\text{O}_2} \qquad (1)$$

(9) The Pd-centered radical in **5** lies in an orbital that is *orthogonal* to the $\pi_{\perp}$* orbital of O_2. This configuration contrasts the "ozone model" that describes Fe−O_2 bonding in hemoglobin. Goddard, W. A.; Olafson, B. D. *Proc. Natl. Acad. Sci. U.S.A.* **1975**, *72*, 2335−2339.
(10) This intermediate exhibits similar O−O bond length and stretching frequency to the recently reported end-on superoxo complex [Cu(Me$_6$-tren)O$_2$]$^+$. Schatz, M.; Raab, V.; Foxon, S. P.; Brehm, G.; Schneider, S.; Reiher, M.; Holthausen, M. C.; Sundermeyer, J.; Schindler, S. *Angew. Chem., Int. Ed.* **2004**, *43*, 4360−4363.
(11) Harvey, J. N.; Aschi, M.; Schwarz, H.; Koch, W. *Theor. Chem. Acc.* **1998**, *99*, 95−99.
(12) The matrix element $\langle ^1\mathbf{7}|H_{SO}|^3\mathbf{7}\rangle$ was estimated using $H_{so} = \xi\mathbf{L}\cdot\mathbf{S}$ with $\xi = 1412$ cm^{-1} for Pd 4d. Only the Pd-based singly occupied Kohn−Sham molecular orbitals corresponding to singlet and triplet wave functions were used in the estimate. For a similar treatment, see: German, E. D.; Efremenko, I.; Sheintuch, M. *J. Phys. Chem. A* **2001**, *105*, 11312−11326. The matrix element is 141 cm^{-1} by INDO-CI computations (see Supporting Information).
(13) Prabhakar, R.; Siegbahn, P. E. M.; Minaev, B. F.; Ågren, H. *J. Phys. Chem. B* **2002**, *106*, 3742−3750.
(14) For example, see: Simándi, L. I. *Catalytic Activation of Dioxygen by Metal Complexes*; Kluwer: Dordrecht, The Netherlands, 1992; Chapter 1, p 8.
(15) (a) Bernardi, F.; Bottoni, A.; Casadio, R.; Fariselli, P.; Rigo, A. *Inorg. Chem.* **1996**, *35*, 5207−5212. (b) Metz, M.; Solomon, E. I. *J. Am. Chem. Soc.* **2001**, *123*, 4938−4950.
(16) For example, see: Bäckvall, J.-E.; Hopkins, R. B.; Grennberg, H.; Mader, M. M.; Awasthi, A. K. *J. Am. Chem. Soc.* **1990**, *112*, 5160−5166.

JA044674B